Crystal Structure of an Ammonium Nickel Molybdate Prepared by Chemical Precipitation

Doron Levin,[†] Stuart L. Soled,[‡] and Jackie Y. Ying*,[†]

Department of Chemical Engineering, Massachusetts Institute of Technology, Cambridge, Massachusetts 02139, and Exxon Research and Engineering Company, Annandale, New Jersey 08801

Received September 15, 1995[⊗]

A layered ammonium nickel molybdate was prepared by precipitation from a solution of nickel nitrate and ammonium heptamolybdate. The compound obtained, $(NH_4)HNi_2(OH)_2(MoO_4)_2$, is trigonal with hexagonal unit cell parameters $a = 6.0147(4)$ Å, $c = 21.8812(13)$ Å, and $Z = 3$. A powder X-ray diffraction pattern was obtained using synchrotron radiation. The structure was generated from three-dimensional Patterson and difference Fourier density maps and refined in the space group $R\bar{3}m$ by the Rietveld method. The structure consists of molybdate tetrahedra and nickel octahedra forming layers perpendicular to the *c* axis. There are three layers per unit cell, with ammonium ions incorporated between the layers. The structure is a member of a solid solution series of $(NH_4)H_{2x}Ni_{3-x}O(OH)(MoO_4)_2$, where $0 \leq x \leq {}^3/_2$. The nonstoichiometry arises from variable occupancy of the nickel position and allows for the formation of these compounds having Ni/Mo ratios varying from 0.75 to 1.5.

Introduction

The solution-based synthesis of first-row transition-metal molybdates yields an interesting array of phases. Pioneering work in this field by Pezerat and co-workers identified a series of phases having ideal formulas $MMoO_4{\cdot}H_2O$, $AHM_2O(MoO_4)_2{\cdot}H_2O$, and $A_{2-x}(H_3O)_xM_2O(MoO_4)_2$,[1−5] where A = NH_4^+, Na^+, or K^+ and M = Zn^{2+}, Co^{2+}, or Ni^{2+}. Preparation of these phases was found to be dependent on the amount of base used, and these phases were designated as Φ_c, Φ_x, and Φ_y, respectively.[1] The crystal structures of phases Φ_x and Φ_y were determined by Pezerat from a limited number of reflections obtained from Weissenberg film data on very small crystals.[4] These materials were shown to exhibit variable and nonstoichiometric compositions. A theory of nonstoichiometry based on cationic and anionic vacancies compensated by the presence of protons was proposed.[4,5] This theory was investigated using phase Φ_x of a compound in which A = K^+ and M = Mg^{2+}.[6−9] However, the limited number of data used in the structure determinations (122 and 147 reflections for the Φ_x and Φ_y crystals, respectively) and the large residuals ($R = 0.09$ for phase Φ_x) raised doubts as to the completeness of the structure determination. For this reason, a fundamental structural study of the phases Φ_x and Φ_y, for the compound in which A = Na^+ and M = Zn^{2+}, was initiated by Clearfield and co-workers about 10 years after the publication of Pezerat's work.[10,11] These studies confirmed the structure of phase Φ_x using a single crystal grown hydrothermally.[10] However, attempts to confirm the structure of phase Φ_y were unsuccessful due to the preparation of an alternate phase resulting from their synthesis conditions.[11] Subsequently, analogs of phase Φ_x, $NaM_2(OH)(H_2O)(MoO_4)_2$ (where M = Mn[12] and Ni[13]), and of the alternate phase $NaM(OH)(MoO_4)$ (where M = Cu[14]) were prepared using reflux and hydrothermal reactions and were characterized. To date, however, no complete crystal structure determination of phase Φ_y has been reported.

Our investigation of the crystal structure of phase Φ_y, however, resulted from an unrelated exploration of the reactivity of metastable mixed-oxide phases. From this work, a novel room-temperature *chimie douce* synthesis technique leading to the preparation of a layered ammonium zinc molybdate has been discovered.[15] In this *chimie douce* reaction, a metastable aluminum-substituted zincite phase, prepared by calcination of Zn/Al layered double hydroxide ($Zn_4Al_2(OH)_{12}CO_3{\cdot}zH_2O$), was reacted with a solution of ammonium heptamolybdate at room temperature to produce a highly crystalline compound.[15] The desire to solve the structure of this unknown material led to the search for a suitable isostructural compound. A search of the JCPDS database identified an isostructural phase (PDF card no. 40-674) reported by Astier,[16] a precipitated powder belonging to a family of "ammonium−amine−nickel−molybdenum oxides". No detailed structural data were given. The *ab initio* crystal structure determination of this ammonium nickel molybdate phase was therefore undertaken.

While the primary motivation for the structure solution of this ammonium nickel molybdate phase resulted from our desire to use it as an isostructural "stepping stone", considerable interest in this phase has been reported in the literature because of its use as a precursor to a nickel molybdate oxidation catalyst.[17−19] Transition-metal molybdates are well-known to

* To whom correspondence should be addressed.
[†] Massachusetts Institute of Technology.
[‡] Exxon Research and Engineering Co.
[⊗] Abstract published in *Advance ACS Abstracts,* June 1, 1996.

(1) Pezerat, H. *C. R. Acad. Sci.* **1965**, *261*, 5490.
(2) Pezerat, H.; Mantin, I.; Kovacevic, S. *C. R. Acad. Sci., Ser. C* **1966**, *262*, 95.
(3) Pezerat, H.; Mantin, I.; Kovacevic, S. *C. R. Acad. Sci., Ser. C* **1966**, *263*, 60.
(4) Pezerat, H. *Bull. Soc. Fr. Mineral. Cristallogr.* **1967**, *90*, 549.
(5) Pezerat, H. *C. R. Acad. Sci., Ser. C* **1967**, *265*, 368.
(6) Peltre, M. J.; Pezerat, H. *J. Less-Common Met.* **1974**, *36*, 61.
(7) Peltre, M. J.; Pezerat, H. *J. Solid State Chem.* **1978**, *23*, 19.
(8) Peltre, M. J.; Olivier, D.; Pezerat, H. *J. Solid State Chem.* **1978**, *24*, 57.
(9) Peltre, M. J.; Pezerat, H. *J. Solid State Chem.* **1978**, *26*, 245.
(10) Clearfield, A.; Sims, M. J.; Gopal, R. *Inorg. Chem.* **1976**, *15*, 335.
(11) Clearfield, A.; Gopal, R.; Saldarriaga-Molina, C. H. *Inorg. Chem.* **1977**, *16*, 628.
(12) Clearfield, A.; Moini, A.; Rudolf, P. R. *Inorg. Chem.* **1985**, *24*, 4606.
(13) Moini, A.; Rudolf, P. R.; Clearfield, A.; Jorgensen, J. D. *Acta Crystallogr.* **1986**, *C42*, 1667.
(14) Moini, A.; Peascoe, R.; Rudolf, P. R.; Clearfield, A. *Inorg. Chem.* **1986**, *25*, 3782.
(15) Levin, D.; Soled, S. L.; Ying, J. Y. *Chem. Mater.* **1996**, *8*, 836.
(16) Astier, M. P.; Dji, G.; Teichner, S. J. *Ann. Chim. (Paris)* **1987**, *12*, 337.

S0020-1669(95)01200-6 CCC: $12.00

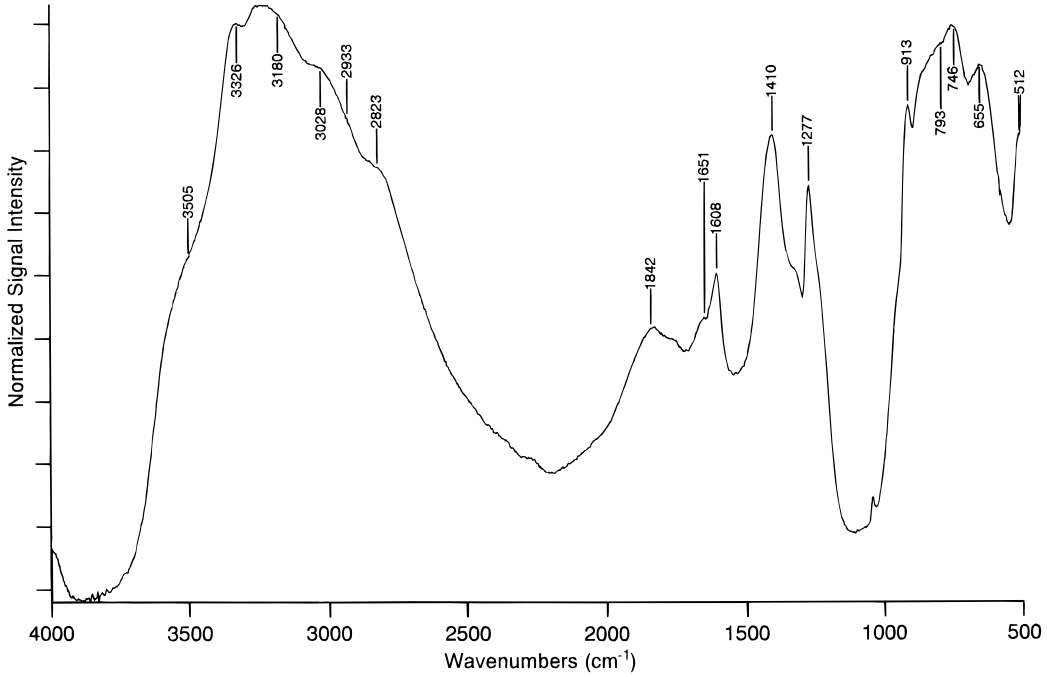

Figure 1. PA-FTIR spectrum of ammonium nickel molybdate.

be catalytically active for partial oxidation reactions, particularly for the selective oxidation of lower alkanes.[19] The transition-metal molybdate oxidation catalysts are typically prepared by calcination of precipitated precursors, an example of which is the ammonium nickel molybdate. In this paper, the full crystallographic structure determination of this precursor, the so-called "green powder",[17,18] is presented.

Experimental Section

Synthesis. The ammonium nickel molybdate was prepared by the method described by Astier.[16] Ammonium heptamolybdate ($(NH_4)_6Mo_7O_{24}\cdot 4H_2O$) and nickel nitrate ($Ni(NO_3)_2\cdot 6H_2O$) were used to prepare a solution containing 0.10 mol of Mo and 0.10 mol of Ni. The initial pH of this green solution was 4.6. The addition of concentrated ammonium hydroxide (28.8% NH_3) precipitated a green solid that dissolved in an excess of ammonia, giving a deep blue solution of pH 8.6. This solution was heated with constant stirring for 4 h, leading to the formation of a pale green precipitate. The pH of the solution just prior to the recovery of the product was 5.6. The product was isolated by vacuum filtration, washed with deionized water, and dried overnight at 110 °C and atmospheric pressure. The product was a fine green powder.

Characterization. (a) Synchrotron X-ray Diffraction. A powder X-ray diffraction pattern was collected on the X-10B beamline at Brookhaven National Laboratory's National Synchrotron Light Source. A Ge(220) monochromator and Ge(111) analyzer were used,[20] and the wavelength was determined to be 1.1278 Å. The direct beam fwhm was equal to 0.0085° and the beam intensity was 1.5E10 photons/s. A flat tray sample holder was used. Data were collected in the range 5−62° 2θ with a step size of 0.015°.

Using the monoclinic cell of Astier,[16] the pattern was indexed and lattice constants were refined by least-squares calculations. Investigation of the relationships between the lattice constants showed that $a \cong b\sqrt{3}$ and $\cos\beta \cong -a/3c$. These relationships suggested that a higher degree of symmetry was present, and the pattern was indexed using a rhombohedral cell on hexagonal axes. The indexed reflections showed systematic absences consistent with the space group $R\bar{3}m$ (No. 166). This symmetry is identical to that reported by Pezerat for phase Φ_y[3] and to that of the rhombohedral layered double hydroxide (LDH) precursor used in the *chimie douce* synthesis of the isostructural ammonium zinc molybdate.[15]

(b) Elemental Analysis. The nickel and molybdenum contents of the powder were determined using X-ray fluorescence (Oneida Research Services, Whitesboro, NY). The metal ratio (Ni/Mo) in the solid, 0.99, agreed well with the Ni/Mo ratio in the starting solution.

(c) Infrared Spectroscopy. The photoacoustic Fourier-transform infrared (PA-FTIR) spectrum of the precipitate is shown in Figure 1. This spectrum was collected with a 2.5 kHz rapid scan at 8 cm^{-1} resolution, using a MTEC Model 200 photoacoustic cell on a Bio-Rad FTS-60A spectrometer. This spectrum confirmed the presence of NH_4^+ ions in the structure, as evidenced by the ν_3 N−H asymmetric stretch in the region 3300−3050 cm^{-1} and the ν_4 H−N−H deformation at 1410 cm^{-1}.[21] The spectrum also shows the presence of an overtone at 2823 cm^{-1} ($2\nu_4$) and a combination band at 3028 cm^{-1} ($\nu_2 + \nu_4$).[21] The broad band in the region 1600−2000 cm^{-1} arises from the interaction of ν_4 with the torsional oscillation ν_6 of the ammonium on its lattice site,[21] suggesting that the ammonium ion is not freely rotating. The PA-FTIR characterization proved that repeated washing of the material could not remove the ammonium ions, leading to the conclusion that the ammonium ions were a part of the crystal structure.

(d) Raman Spectroscopy. The Raman spectrum of the precipitate, collected with a Bio-Rad FT-Raman spectrometer, is shown in Figure 2. The excitation source was a Nd-YAG laser operated at 1064 nm with input power of 60 mW. The signal was detected with a liquid-nitrogen-cooled Ge detector. The Raman spectrum is relatively simple and confirmed the tetrahedral coordination of the molybdate anion. The two strong bands at 904 and 321 cm^{-1} were assigned to a ν_1 symmetric stretch and a ν_2 symmetric bend, respectively.[22] The presence of only one symmetric stretch suggested that the molybdenum was occupying a single crystallographic tetrahedral site.

Refinement and Solution of Structure. A least-squares refinement of the peak positions gave an initial hexagonal unit cell with parameters $a = 6.01$ Å and $c = 21.87$ Å. With this cell, the initial molybdenum and nickel atom positions were identified using three-dimensional Patterson methods. The oxygen and nitrogen atoms were then found

(17) Mazzocchia, C.; Kaddouri, A.; Anouchinsky, R.; Sautel, M.; Thomas, G. *Solid State Ionics* **1993**, *63*, 731.
(18) Mazzocchia, C.; Anouchinsky, R.; Kaddouri, A.; Sautel, M.; Thomas, G. *J. Therm. Anal.* **1993**, *40*, 1253.
(19) Mazzocchia, C.; Aboumrad, C.; Diagne, C.; Tempesti, E.; Herrmann, J. M.; Thomas, G. *Catal. Lett.* **1991**, *10*, 181.
(20) Cox, D. E.; Hastings, J. B.; Thomlinson, W.; Prewitt, C. T. *Nucl. Instrum. Methods* **1983**, *208*, 573.
(21) Waddington, T. C. *J. Chem. Soc.* **1958**, 4340.
(22) Sheik Saleem, S.; Aruldhas, G.; Bist, H. D. *J. Solid State Chem.* **1983**, *48*, 77.

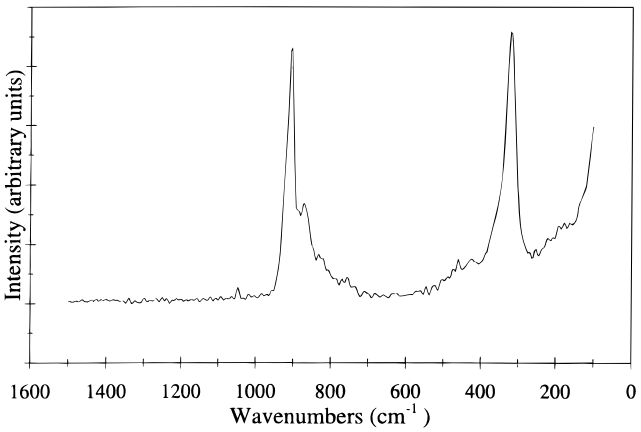

Figure 2. FT-Raman spectrum of ammonium nickel molybdate.

using successive difference Fourier syntheses. The model was refined by the Rietveld method using the General Structure Analysis System (GSAS).[23] The refinement included scale, background, lattice parameters, zero-point error, the Gaussian profile, the Lorentzian profile, asymmetry, anisotropic peak broadening, atom positions, nickel site occupancy, and thermal parameters. Isotropic temperature parameters were used for oxygen and nitrogen and anisotropic temperature parameters for molybdenum and nickel. X-ray anomalous dispersion coefficients were calculated using FPRIME within GSAS.[23] No corrections were made for absorption or extinction.

The refinement converged with $\mathbf{R}_{wp} = 13.5\%$ and $\mathbf{R}_p = 10.4\%$. The data, fit, and residuals are shown in Figure 3. The atomic positions and thermal parameters are listed in Table 1, and the summary of the refinement parameters is given in Table 2. The main concern over the refined parameters resulted from the low value of the nickel occupancy. This value, 0.575(6), is a bit far from the theoretical value of 0.667. The most significant residual occurs for the (101) peak at 12.8° 2θ, probably due to preferred orientation causing the observed intensity to be significantly larger than the calculated intensity. In an attempt to reduce the residual of this peak, the refinement program reduced the nickel occupancy factor until further reductions were offset by increased residuals at other peaks. However, attempts to correct for preferred orientation using GSAS did not result in a significant improvement in the overall fit or lead to a significant increase in the nickel occupancy.

Consistency Check of Determined Structure. The bond-valence method[24−26] was used to check whether the determined Mo−O and Ni−O bond distances support valencies of +6 and +2 for the Mo and Ni, respectively. For Mo^{VI}−O and Ni^{II}−O bonds, values of $R = 1.907$ Å and $R = 1.654$ Å, respectively, were used.[25] Using the values for d_{Ni-O} and d_{Mo-O} presented in Table 3, the valencies of the molybdenum and nickel atoms were calculated as +7.06 and +1.77, respectively. These calculated values differ from the assumed valencies of +6 and +2 by +17.7% and −11.5% respectively. These error margins correspond to a combined error of about ±0.05 Å in R_{ij} and the bond length. As the reported accuracy of R_{ij} is ±0.02 Å,[25] the determined crystal structure is consistent.

Description of Structure

The framework of the ammonium nickel molybdate consists of sheets of distorted nickel octahedra to which tetrahedral molybdate groups are bonded. These layers are stacked in the *c* direction and are held together by hydrogen bonding. The nickel atoms defining these layers are located at site 9(e) which has variable occupancy ranging from $^1/_2$ to 1. If the occupancy of this site is 1, the arrangement of nickel atoms can be considered as a pattern of two alternating strings, one being Ni−Ni−Ni and the other being Ni−□−Ni, where □ represents an ordered cation vacancy. This ordered cation vacancy is independent of the nickel occupancy. As the nickel occupancy deviates from unity, additional disordered vacancies appear in both strings. For the compound studied, the Ni/Mo ratio is 1 and three of every nine nickel sites are vacant. The coordination of oxygens about the nickel atoms is distorted octahedral, with a tetragonal contraction along the C_4 axis running through O(1)−Ni−O(1). The bond distances and angles defining the distorted octahedra are shown in Tables 3 and 4. The nickel atoms are linked to each other through double oxygen bridges. Each nickel octahedron shares edges with a maximum of four adjacent octahedra, thereby creating the sheets of octahedra perpendicular to the *c* axis.

The absence of a nickel atom at the origin generates ordered vacancies in the sheet. These ordered vacant octahedral sites are capped, both above and below, by tetrahedral molybdate groups. Disordered vacant octahedral sites resulting from a reduction in the nickel occupancy from unity are, however, not capped by tetrahedral molybdate groups. The molybdate tetrahedra above and below an ordered vacancy are related to each other by an inversion center midway between them. The tetrahedra share three of their corners with the nickel−oxygen octahedra at O(3). Since there are four O(3) atoms in each octahedron, four octahedral corners are shared with four different molybdate tetrahedra. Each molybdate tetrahedron shares corners with six different nickel octahedra, generating the hexagonal arrangement shown in Figure 4.

The three nickel molybdate layers defining the unit cell are stacked at a separation of $c/3 = 7.2938(12)$ Å. In these layers, the position of the permanently vacant octahedral site capped by the molybdate groups follows the sequence *A*−*B*−*C*−*A* (where *A*, *B*, and *C* are the three 3-fold axes at $x,y = 0,0$; $^2/_3,^1/_3$; and $^1/_3,^2/_3$). This three-layer arrangement is shown in Figure 5. Between each layer, in the space defined by O(3) oxygens of six tetrahedral molybdates, lie ammonium ions. The positions of the nitrogen atoms follow the sequence *C*−*A*−*B*−*C*. The N−O(3) distance of 2.98 Å suggests that the ammonium ions are oriented with three of the four hydrogens directed toward O(3), thereby anchoring the ammonium ion via a hydrogen-bonding mechanism. The arrangement of O(3) atoms is symmetrically equivalent above and below the nitrogen, suggesting that two orientations for the ammonium ions are possible. The ammonium ions can likely be found in either orientation with equal probability. The restriction on the orientation of the ammonium ions is supported by the infrared spectroscopic analysis that suggested that the ammonium ions are not freely rotating. The ammonium ions do not serve to connect the array of layers in the [001] direction, the N−O(1) distance of 4.49 Å being too long for hydrogen bonding. The vertical distance between O(2), the apical oxygen of the molybdate tetrahedra, and O(1), the bridging oxygen of the adjacent nickel layer, is 2.88 Å, suggesting that these two oxygens are involved in hydrogen bonding via hydroxyl protons that serves to connect the layers. Figure 6 illustrates a three-dimensional polyhedral representation of the crystal structure.

Assignment of Hydrogen Atoms

The non-hydrogen elements of the unit cell, as determined by elemental analysis and the refinement of the powder X-ray data, suggested an initial formula for this compound as "$(NH_4)_3Ni_6O_6(MoO_4)_6$". However, inspection of this formula shows that an additional 9 hydrogen atoms must be present to ensure charge balance. In the compound "$(NH_4)_3H_9Ni_6O_6(MoO_4)_6$",

(23) GSAS, General Structure Analysis System, Larson, A. C.; von Dreele, R. B., LANSCE, Los Alamos National Laboratory, copyright 1985−1994 by the Regents of the University of California.
(24) O'Keeffe, M. *Struct. Bonding* **1989**, *71*, 162.
(25) Brese, N. E.; O'Keeffe, M. *Acta Crystallogr.* **1991**, *B47*, 192.
(26) O'Keeffe, M.; Brese, N. E. *J. Am. Chem. Soc.* **1991**, *113*, 3226.

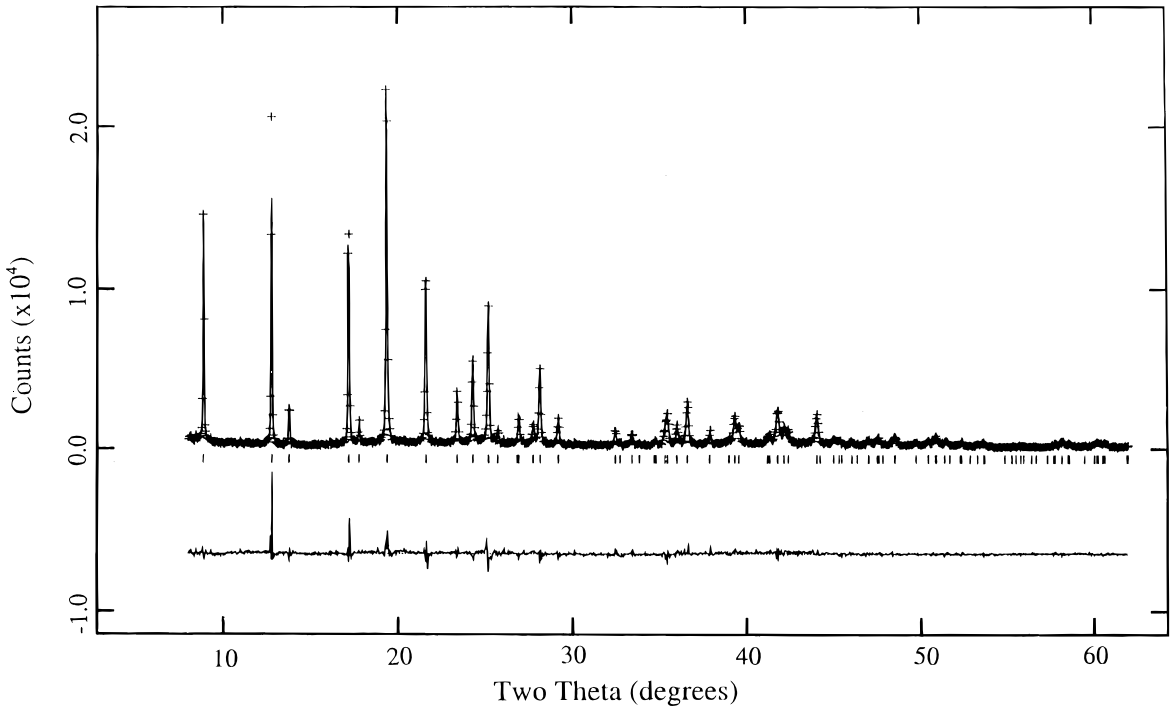

Figure 3. Synchrotron powder X-ray data, including Rietveld fit and residuals for $(NH_4)HNi_2(OH)_2(MoO_4)_2$. The set of short vertical bars below the data set indicate the positions of possible Bragg reflections.

Table 1. Final Positional and Thermal Parameters (Å^2)

atom	Wyckoff posn	*x*	*y*	*z*	10^2U_{iso}	fraction
Mo	6(c)	0	0	0.08850(10)	5.7[a]	1.0
Ni	9(e)	$^1/_2$	0	0	4.1[b]	0.575(6)
O(1)	6(c)	0	0	0.2952(6)	6.8(5)	1.0
O(2)	6(c)	0	0	0.1636(7)	9.6(7)	1.0
O(3)	18(h)	0.3072(14)	0.1536(7)	−0.06067(29)	6.9(3)	1.0
N	3(b)	0	0	$^1/_2$	4.1(6)	1.0

[a] $10^2(U_{11} = U_{22}) = 7.0(2)$, $10^2U_{33} = 3.1(2)$, $10^2U_{12} = 3.47(8)$, $U_{13} = U_{23} = 0$. [b] $10^2U_{11} = 3.8(3)$, $10^2U_{22} = 5.3(4)$, $10^2U_{33} = 3.2(3)$, $10^2U_{12} = 2.6(2)$, $10^2U_{13} = -0.09(14)$, $10^2U_{23} = -0.17(28)$.

Table 2. Crystallographic Data for $(NH_4)HNi_2(OH)_2(MoO_4)_2$ from THE Rietveld Refinement of Powder X-ray Diffraction Data

powder color	pale green	*V* (Å^3)	685.53(7)
formula	$(NH_4)HNi_2(OH)_2(MoO_4)_2$	*Z*	3
fw	490.34	D_{calc} (g/cm^3)	3.446
space group	$R\bar{3}m$	$\mathbf{R}_{wp}$ (%)	13.5
a (Å)	6.0147(4)	$\mathbf{R}_p$ (%)	10.4
c (Å)	21.8812(13)	$\mathbf{R}_{exp}$ (%)	2.2

Table 3. Selected Interatomic Distances (Å)

	Bonded		
Mo−O(2)	1.643(14)	Ni−O(1) (×2)	1.926(5)
Mo−O(3) (×3)	1.712(7)	Ni−O(3) (×4)	2.243(5)
	Nonbonded		
Mo−Mo (across layer)	3.873(13)	N−O(1)	4.486(13)
Ni−Ni (between adjacent layers)	7.294(13)	N−O(2)	3.473(3)
		N−O(3)	2.981(6)
O(2)−O(1)	2.880(18)		

Table 4. Selected Interatomic Angles (deg)

O(2)−Mo−O(3) (×3)	110.83(23)	Ni−O(1)−Ni (×3)	102.7(4)
O(3)−Mo−O(3) (×3)	108.08(24)		

there are 21 hydrogen atoms to be placed in the unit cell, 9 of which are associated with the nickel−molybdenum−oxygen framework, the balance belonging to ammonium ions. The positions of the hydrogen atoms were tentatively determined by considering the crystal chemistry in regions of residual electron density (~1 e/Å^3) in the difference Fourier maps.

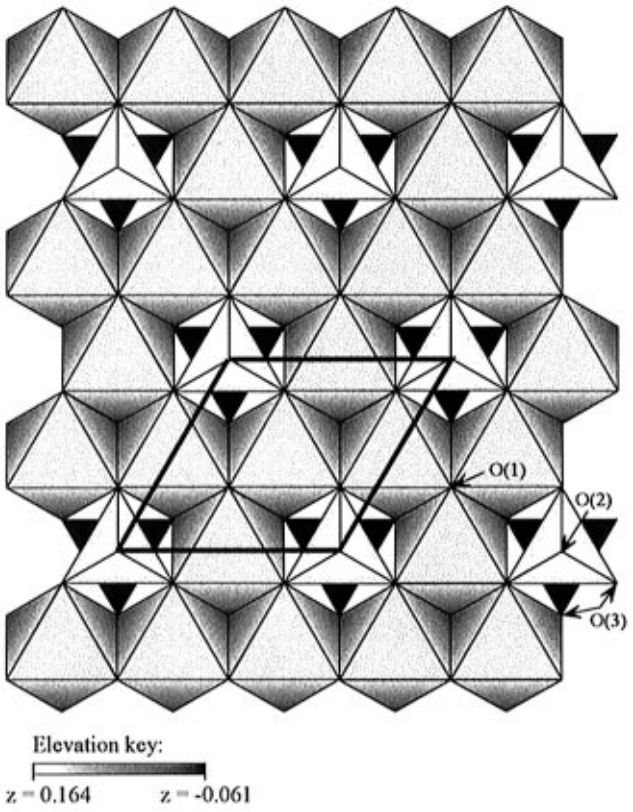

Figure 4. Basal plane of $(NH_4)HNi_2(OH)_2(MoO_4)_2$, viewed along [001].

The positions of the hydrogen atoms of the ammonium groups (H(1) and H(2)) were determined by calculation using a N−H distance of 1.03 Å[27] and are shown in Table 5. It appears that two possible orientations of the ammonium ions are possible, as inferred from crystallographic and PA-FTIR analysis. The

(27) Gutowsky, H. S.; Pake, G. E.; Bersohn, R. *J. Chem. Phys.* **1954**, *22*, 643.

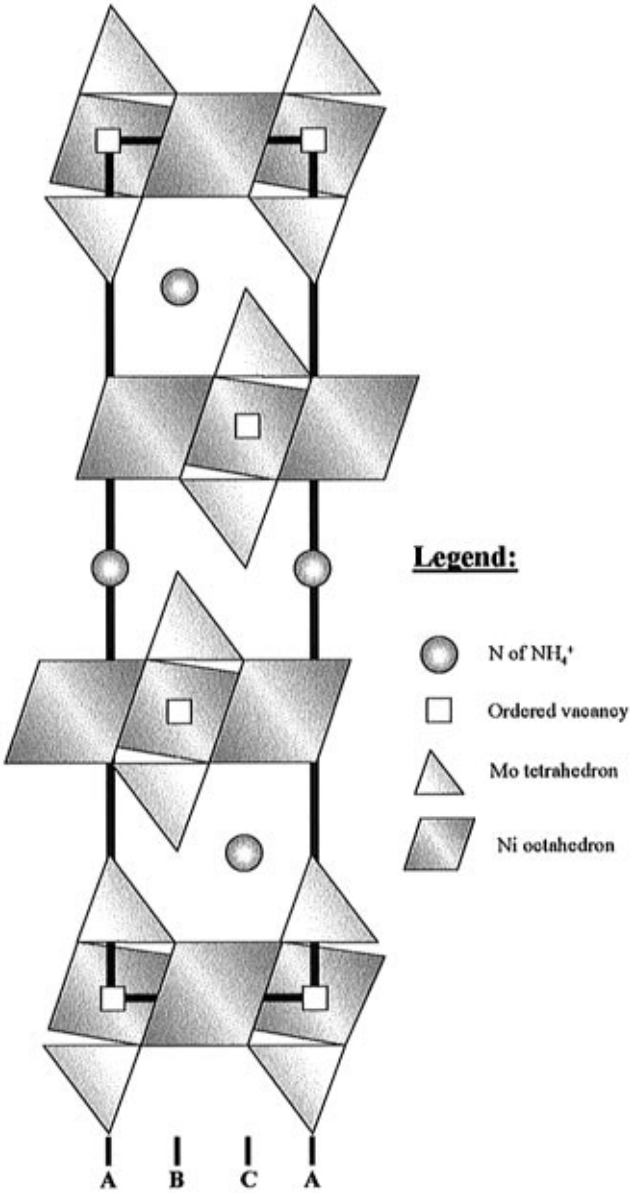

Figure 5. Crystal structure of $(NH_4)HNi_2(OH)_2(MoO_4)_2$, viewed along [010], showing three-layer arrangement in polyhedral representation.

coordination of O(3) oxygens around the nitrogen is octahedral with a N−O(3) distance of 2.98 Å. On the basis of the PA-FTIR analysis that showed the ammonium ions not rotating freely, it was surmised that the ammonium ions are tethered by hydrogen bonds between N−H and O(3). Consequently, the hydrogen atom H(2) was placed along the line joining N and O(3), at a distance of 1.03 Å from the nitrogen. Since the arrangement of O(3) atoms is symmetrically equivalent above and below the nitrogen atom, occupancies of $^1/_2$ were assigned to H(1) and H(2) to account for the equal probability of finding the ammonium ion in either orientation.

An additional 9 hydrogens needed to be assigned to the nickel−molybdenum−oxygen framework to ensure charge balance. The presence of a strong O−H stretching band in the PA-FTIR spectrum suggested that the bridging oxygen O(1) acts as a bridging hydroxyl. The O(1)−O(2) distance of 2.88 Å is also indicative of possible hydrogen bonding in the [001] direction that could serve to connect the layers. The hydrogen atom H(3) was therefore placed in a position such that the O(1)−H(3) distance is 0.97 Å.[28] The location of a hydrogen atom at

(28) Ichikawa, M. *Acta Crystallogr.* **1978**, *B34*, 2074.

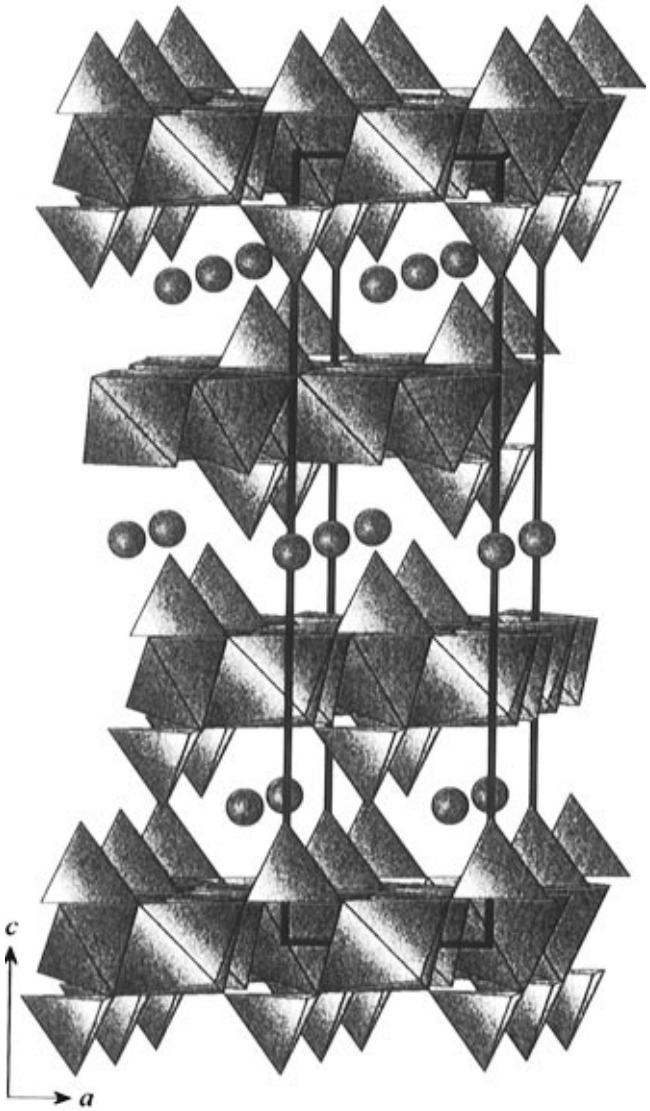

Figure 6. Crystal structure of $(NH_4)HNi_2(OH)_2(MoO_4)_2$, viewed in polyhedral representation.

Table 5. Calculated Hydrogen Positions

atom	Wyckoff posn	*x*	*y*	*z*	fraction
H(1)	6(c)	0	0	0.4529	$^1/_2$
H(2)	18(h)	0.2711	0.5422	0.1301	$^1/_2$
H(3)	6(c)	0	0	0.2506	1
H(4)	6(c)	0	0	0.3430	$^1/_2$

this site with full occupancy (Table 5) accounts for 6 of the 9 hydrogens in the framework and makes all the bridging O(1) atoms bridging hydroxyls.

It is interesting to compare the difference Fourier maps before and after the placement of these hydrogens. A difference Fourier map of the partial (010) plane, calculated before the placement of the hydrogens, is shown in Figure 7. In addition to the residual density at the site of the heavy molybdenum atom, there are three crystallographically independent regions of positive electron density (∼1 e/Å^3), designated in Figure 7 as ρ_1, ρ_2, and ρ_3. The region of electron density ρ_1 corresponds to the H(1) hydrogen of the ammonium group centered at 0, 0, $^1/_2$. The symmetry-equivalent position above the nitrogen is clearly visible in Figure 7. The other hydrogens (H(2)) forming the ammonium group are not in the plane shown in Figure 7.

The region of electron density ρ_2 corresponds to the H(3) hydrogen belonging to O(1). It was the presence of this residual

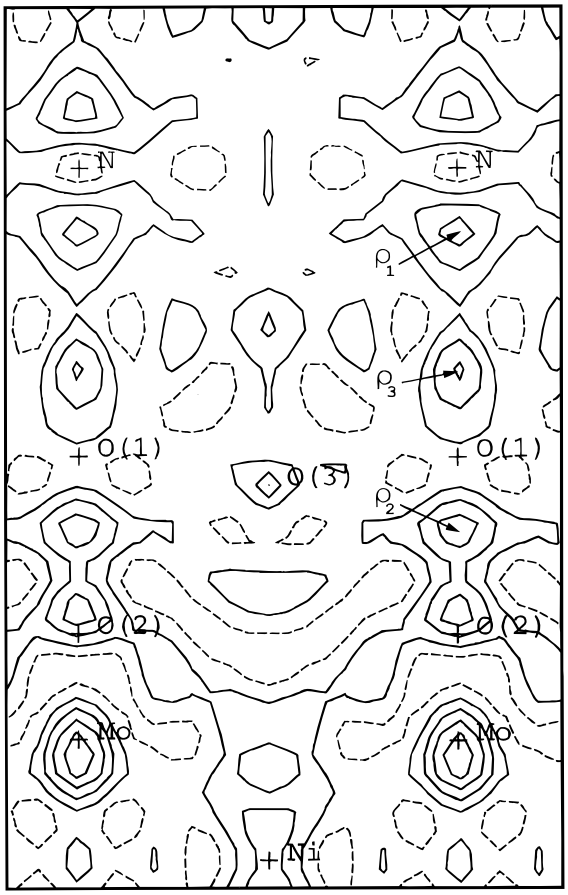

Figure 7. Difference Fourier map showing partial (010) plane. Successive contour lines differ by 0.3 e/Å^3. Dashed contours are negative.

electron density in the difference Fourier map that suggested that O(1) acts as bridging hydroxyl group for the hydrogen bonding between O(1) and O(2). An alternative location for the H(3) hydrogen, closer to O(2) along the line joining O(1) and O(2), would make the apical molybdate oxygen a hydroxyl, leading to the possible chemical formula $(NH_4)HNi_2O_2(MoO_3OH)_2$. There was, however, no experimental evidence to support this model which was therefore rejected. With the H(3)−O(1) distance set at 0.97 Å, the H(3)···O(2) distance of 1.90 Å is consistent with hydrogen bonding linking adjacent nickel molybdate layers through the interaction of the apical molybdate oxygen with the bridging hydroxyl.

An additional 3 hydrogens needed to be placed in the nickel−molybdenum−oxygen framework of the unit cell to ensure charge balance. The excellent correspondence between the observation of residual electron density at the sites calculated to contain hydrogens led to the speculation that the region ρ_3 could also be indicative of the location of hydrogens. This region of residual electron density ρ_3 corresponds to a tetrahedral site with point symmetry 3*m* associated with the O(1) oxygen. This region of residual electron density was, therefore, tentatively assigned to a hydrogen, designated H(4), occupying this tetrahedral site. This arrangement is shown in Figure 8a. An alternative location for these remaining hydrogens is shown in Figure 8b. In this alternative model, half the bridging O(1) oxygens would be bridging waters and the remainder bridging hydroxyls, giving a possible chemical formula of $(NH_4)Ni_2OH(H_2O)(MoO_4)_2$. The presence of an H−O−H bending vibration band in the PA-FTIR spectrum cannot support the model shown in Figure 8b since the same band appears for the compound having full occupancy of the nickel site, i.e. $(NH_4)Ni_3O(OH)(MoO_4)_2$.[29] (As indicated in the Discussion, a compound having full occupancy of the nickel site has only 3 framework hydrogens, making half the bridging oxygens hydroxyls.) It is the presence of surface-adsorbed water on the compound that gives rise to the H−O−H bending mode in the PA-FTIR spectrum. The assignment of hydrogens in the manner discussed above led to the chemical formula for this compound as $(NH_4)HNi_2(OH)_2(MoO_4)_2$.

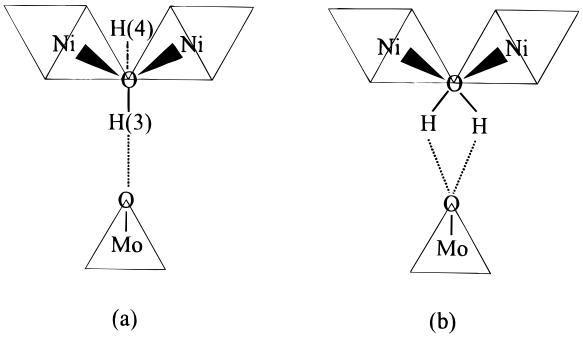

Figure 8. Possible locations for framework hydrogens: (a) in tetrahedral site associated with bridging hydroxyl; (b) as bridging water.

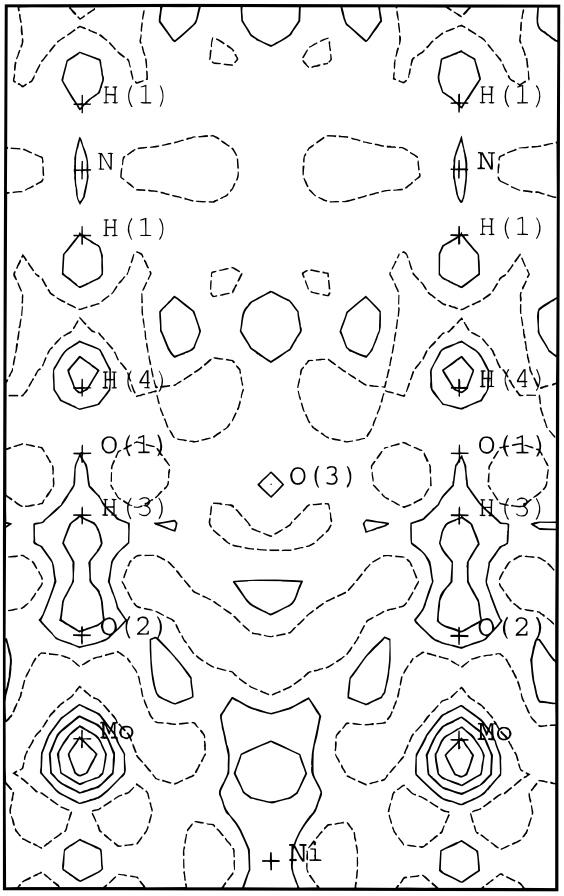

Figure 9. Difference Fourier map showing partial (010) plane. Successive contour lines differ by 0.3 e/Å^3. Dashed contours are negative. The difference Fourier map was calculated for $\mathbf{R}_{wp} = 13.5\%$, $\mathbf{R}_p = 10.4\%$.

Accurate refinement of these hydrogen positions is not possible with powder X-ray data. However, using the calculated hydrogen positions, a final difference Fourier map was calculated using a default thermal parameter of 0.025 Å^2 for the hydrogen atoms and is shown in Figure 9. This figure illustrates

(29) Levin, D. Unpublished results.

Table 6. Variables Defining the Compositions of Structures Having the General Formula $(NH_4)H_{2x}Ni_{3-x}O(OH)(MoO_4)_2$

x	Ni/Mo ratio	Ni site occ	fraction of O(1) as hydroxyl	proton occ of T_2 site[a]	formula
0.0	1.5	1	$^1/_2$	0	$(NH_4)Ni_3O(OH)(MoO_4)_2$
0.5	1.25	$^5/_6$	1	0	$(NH_4)Ni_{2.5}(OH)_2(MoO_4)_2$
1.0	1.0	$^2/_3$	1	$^1/_2$	$(NH_4)HNi_2(OH)_2(MoO_4)_2$
1.5	0.75	$^1/_2$	1	1	$(NH_4)H_2Ni_{1.5}(OH)_2(MoO_4)_2$

[a] T_2 site = tetrahedral site having point symmetry 3*m*.

that the only remaining residual electron density greater than 0.5 e/Å^3 is associated with the heavy molybdenum atom.

Discussion

On the basis of the structure of $(NH_4)HNi_2(OH)_2(MoO_4)_2$ as described above, we are proposing that this material is a member of a solid solution series of $(NH_4)H_{2x}Ni_{3-x}O(OH)(MoO_4)_2$, where $0 \leq x \leq 3/2$. The nonstoichiometry arises from variable occupancy of the nickel position. The nickel atom is situated at position 9(e), and we are proposing that the occupancy of this site can vary from $^1/_2$ to 1. Since molybdenum sits at site 6(c) with full occupancy, the Ni/Mo ratio should theoretically be able to vary from 0.75 to 1.5.

The preparation of this compound with various Ni/Mo ratios has been carried out by Astier.[16] Even with solutions having atomic Ni/Mo ratios varying from 0.25 to 2.0, the final precipitated solids contained experimentally determined Ni/Mo ratios only between 0.8 and 1.6.[16] The structure now explains this composition range. The compounds having the general formula $(NH_4)H_{2x}Ni_{3-x}O(OH)(MoO_4)_2$ with $x = 0$, 0.5, 1 and 1.5 were chosen as examples to illustrate this solid solution series. All the necessary crystallographic variables are summarized in Table 6.

The upper limit to the Ni/Mo ratio is set by the maximum occupancy of the Ni site. The maximum Ni/Mo ratio occurs at full nickel occupancy, giving a Ni/Mo ratio of 1.5. In this compound, $(NH_4)Ni_3O(OH)(MoO_4)_2$, half the bridging O(1) atoms would be hydroxyls, the remainder being oxygen. There are also no additional associated H(4) hydrogens. As the occupancy of the nickel position decreases, the number of hydrogens should increase to maintain charge balance. The additional hydrogens initially convert the bridging O(1) oxygens into hydroxyls, such that, at a nickel occupancy of $^5/_6$, all the bridging O(1) oxygens are hydroxyls. Any further decrease in the nickel occupancy would then lead to the incorporation of associated H(4) hydrogens.

As shown in Figure 10, the two layers of four close-packed oxygens contained within the unit cell area generate 4 octahedral sites and 8 tetrahedral sites. The four octahedral sites are occupied by $3 - x$ nickel atoms, one ordered vacancy (shown in Figure 10 as □), and x disordered vacancies. The eight tetrahedral sites consist of two groups: six sites having point symmetry *m*, designated T_1, and two sites having point symmetry 3*m*, designated T_2. We are proposing that only the T_2 sites accommodate the associated hydrogens.

The structure determined in this paper, $(NH_4)HNi_2(OH)_2(MoO_4)_2$, corresponds to the compound with $x = 1$. In this compound, the occupancy of the nickel site is $^2/_3$, giving a Ni/Mo ratio of 1. To ensure charge balance, all the bridging O(1) atoms are hydroxyls and half the T_2 sites contain associated hydrogens. The minimum Ni/Mo ratio occurs at a nickel occupancy of $^1/_2$, giving a Ni/Mo ratio of 0.75. In this compound, $(NH_4)H_2Ni_{1.5}(OH)_2(MoO_4)_2$, all the bridging O(1) atoms would be hydroxyls and each would have an associated hydrogen accommodated in its tetrahedral site, T_2. At this Ni/Mo ratio, all the tetrahedral sites having point symmetry 3*m* would be occupied by hydrogens. We are therefore proposing that the minimum in the Ni/Mo ratio is set by the inability of the structure to accommodate any more hydrogens required for charge balancing. These proposals are currently being verified. A deuterated analog of the title compound, $(ND_4)DNi_2(OD)_2(MoO_4)_2$, is being investigated using neutron diffraction. ^{1}H solid-state NMR studies are also underway. These studies will be presented in a future paper.

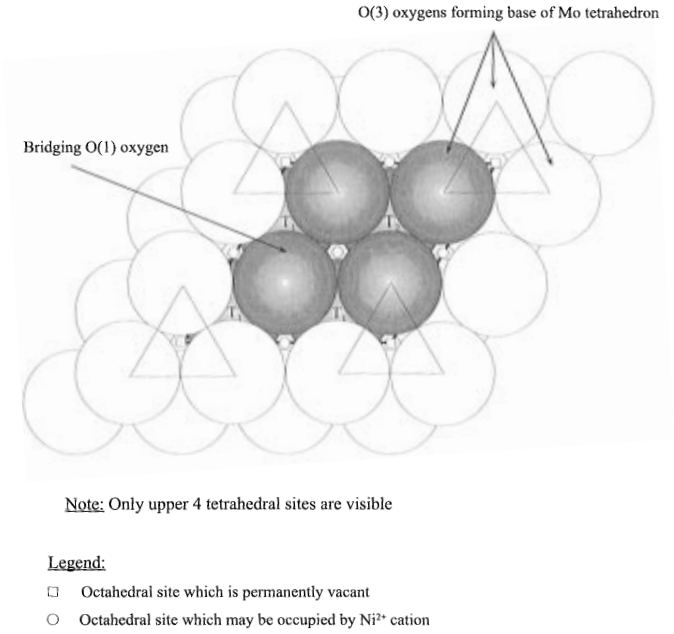

Figure 10. Arrangement of tetrahedral and octahedral sites within the unit cell area.

Conclusions

Our investigation into the crystal structure determination of phase Φ_y had resulted from our desire to solve the structure of an unknown material generated by the reaction of a metastable aluminum-substituted zincite phase with a solution of ammonium heptamolybdate.[15] This material is isostructural with the ammonium nickel molybdate $(NH_4)HNi_2(OH)_2(MoO_4)_2$, the *ab initio* crystal structure determination of which is presented in this paper. Knowledge of the crystal structures shows these ammonium transition-metal molybdates to be isostructural with Pezerat's phase Φ_y and verifies his structure determination. Our analysis of this phase confirms the presence of nonstoichiometry in the divalent transition-metal cation content. However, we find no evidence for the other cationic and anionic vacancies proposed by Pezerat to exist in this structure.

Acknowledgment. This work was funded by the National Science Foundation (Grant CTS-9257223). D.L. was partially supported by the Exxon Summer Intern Program. We acknowledge B. Zhang (Exxon) for collecting the synchrotron data set and T. Sun (MIT) for the Raman spectrum and are grateful to M. E. Leonowicz and B. J. Wuensch, D. S. Bem, and J. D. Houmes (MIT) for assistance with GSAS and useful discussions.

Supporting Information Available: Table S1, listing bond distances and bond angles between all possible combinations of atoms, and Table S2, giving the observed and calculated GSAS refinement (5 pages). Ordering information is given on any current masthead page.

IC951200S